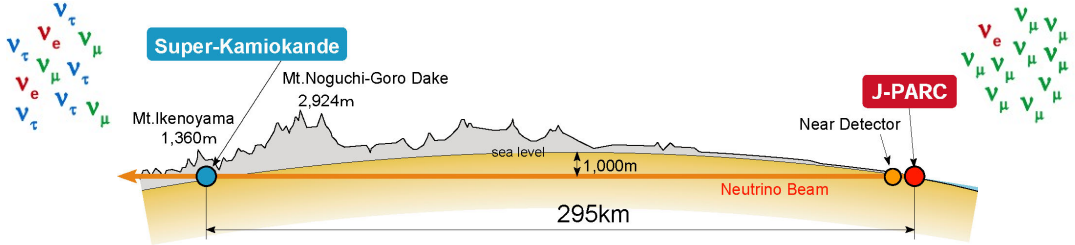
T2K and Hyper-K status

11th French-Ukrainian workshop on the instrumentation developments for HEP

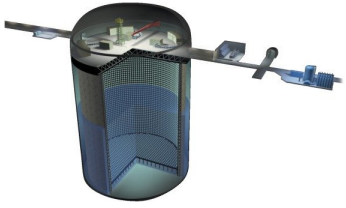
Guillaume EURIN

October 14, 2026

Tokai-to-Kamioka: T2K long-baseline experiment

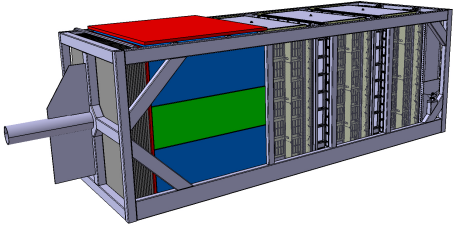


- Far site: Water-Cherenkov Super-Kamiokande



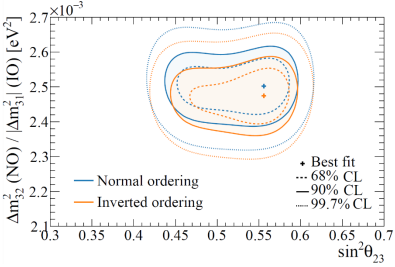
- SK (22 kt) to be replaced by HK (190 kt)

- Near detector suite: INGRID and ND280

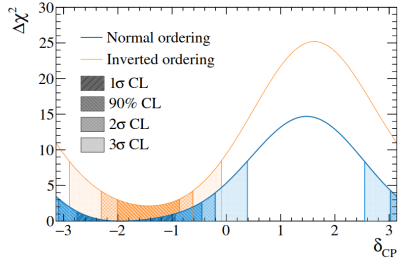


- Upgrade of ND280 performed in 23/24
  $\Rightarrow$ sFGD/HA-TPCs/ToF

Current T2K results



PRL 135, 261801 (2025)

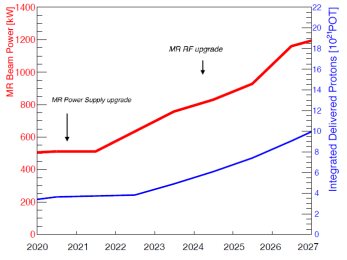


Nature 580, 339–344 (2020)



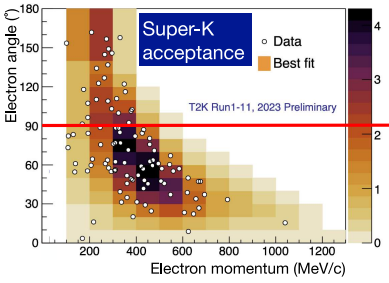
- Indication of CP-violating value of δ_{CP} around $-\frac{\pi}{2}$
- More statistics needed: beam upgrade
  Proton beam power above 1 MW
- Improved systematic uncertainty: ND280 upgrade

T2K Projected POT (Protons-On-Target)

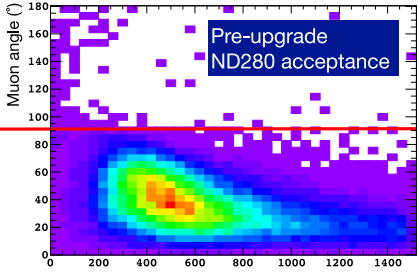


Motivation for the upgrade of ND280

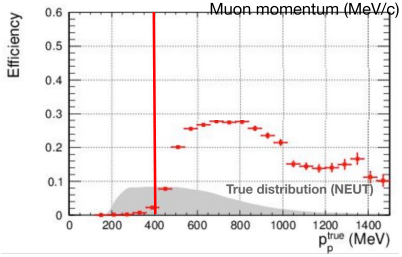
Super - Kamiokande



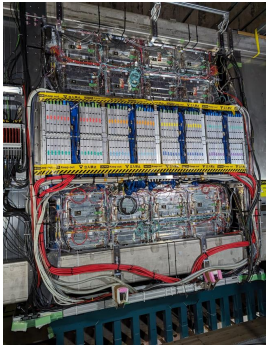
ND 280

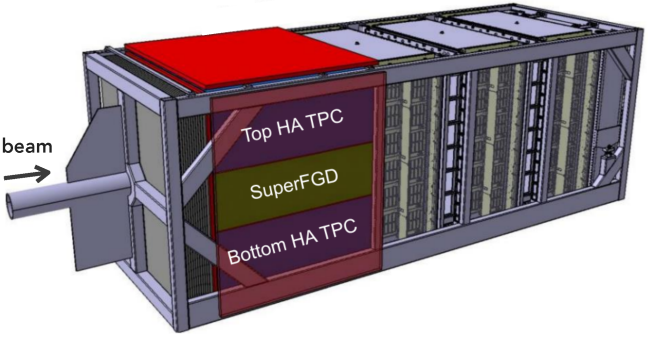


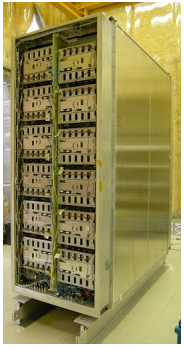
- Limited angular acceptance for final state muons at ND 280
- Limited efficiency for low energy protons



TPCs for the near detector of T2K-ND280



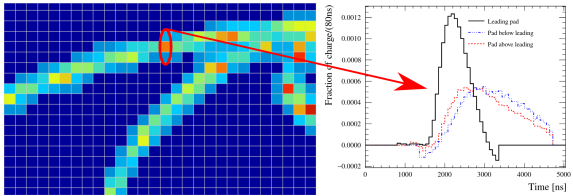


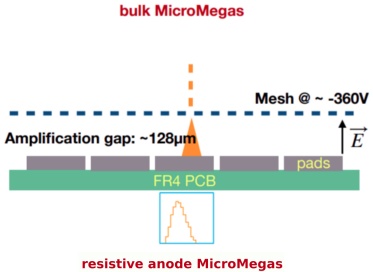


- 1998: TPC studies conducted for ILC with Micromegas R&D
- 2009: 3 vertical TPCs with 72 bulk Micromegas ($\sim$ 9 m^2)
- 2017: Encapsulated Resistive Anode bulk Micromegas (ERAM) proposed for T2K ND280-Upgrade
- 2024: 2 High-Angle TPCs with 36 ERAM detectors installed ($\sim$ 5 m^2)

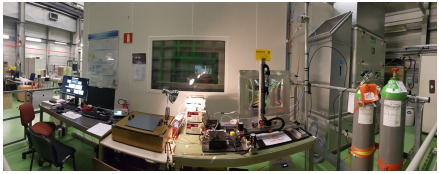
Encapsulated Resistive Anode bulk Micromegas (ERAM)

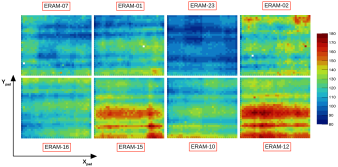
- Bulk Micromegas, with resistive Diamond-Like Carbon.
- Charge spreading over multiple pads (ILC-TPC R&D) for spatial resolution improvement.





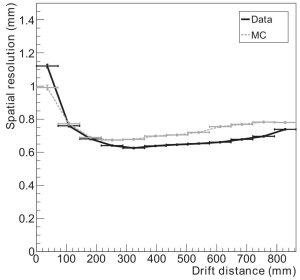
- Test bench with ^{55}Fe source to characterize all ERAMs (NIM-A.2023.168534)



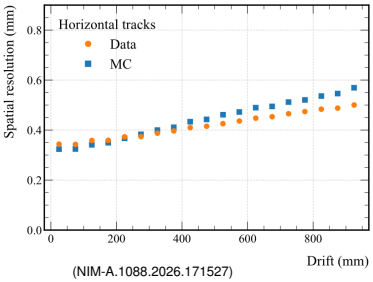


High Angle TPCs

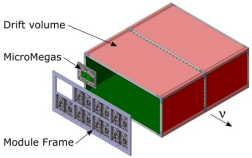
Vertical TPCs

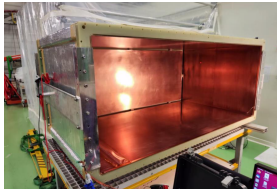


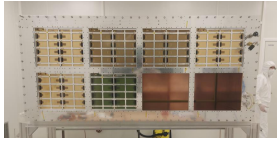
High-Angle TPCs



(NIM-A.1088.2026.171527)



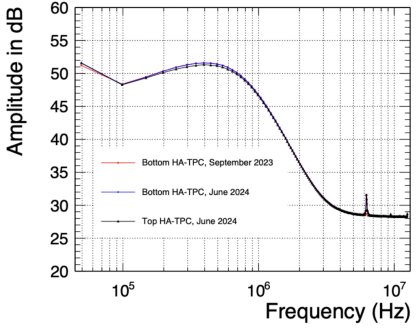




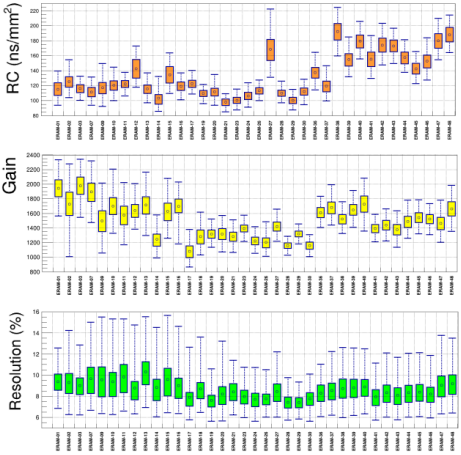
- Particle identification through dE/dx:
  Energy resolution: $\sim$ 10 % (PID: 45 % larger dE/dx for e^- than μ/π)
- Technology tested on test beams at DESY (NIM-A.2023.168248) and CERN

Systematic characterisation of the ERAM detectors

- Main characteristics of ERAMs systematically studied
- Populations: design evolution, production parameters
- Detectors grouped with performances for installation
- Precise characterization of detector effects:

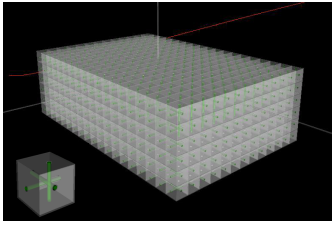


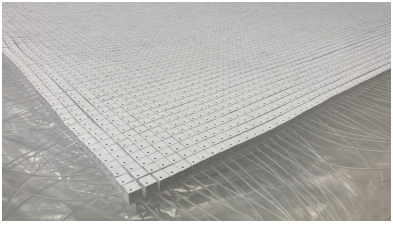
NIM-A 2023.168534



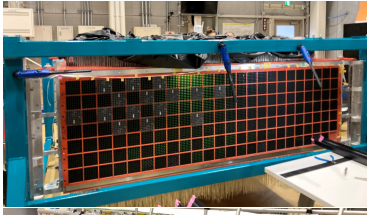
Thesis of Shivam Joshi

Super Fine Grained Detector





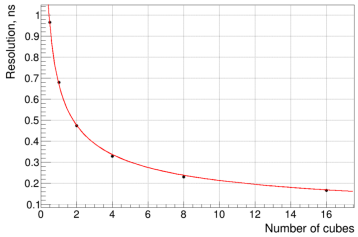


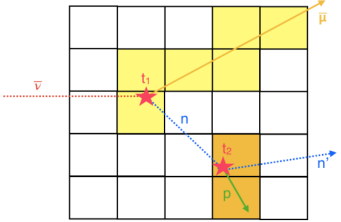


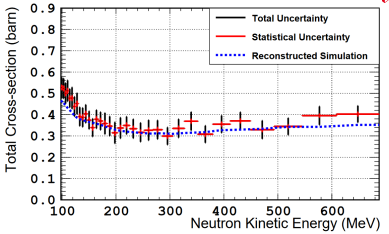


- $2{\times}10^6$ scintillator cubes 1cm$\times$1cm$\times$1cm with 3 holes (x, y, z)
- WLS fibers readout with $\sim$ 56 000 MPPC
- Etched surfaces for optical insulation
- Active mass $\sim$ 2 tons

Super Fine Grained Detector



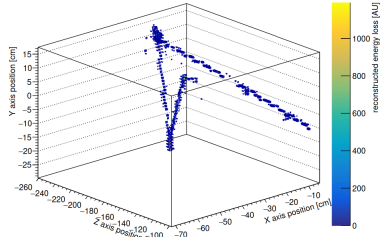




JINST 18 (2023) 01, P01012

Phys. Let. B 2023 137843

Run = 16846, subrun = 0, event = 6430

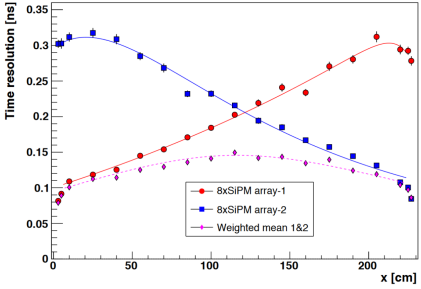


- Several prototypes in laboratory and on beams (charged particles and neutrons)
- Time resolution measured on beam at 0.97 ns per channel
- Neutron detection via proton recoil and neutron energy from time-of-flight
- Tracking capability and e^-/photon separation

Time of Flight detector

- Precise timing of final state particles
- Together with SFGD timing separate in-outgoing particles
- Particle identification using timing
- Cosmic trigger for the calibration of inner detectors
- 150 ps timing resolution reached during commissioning at CERN



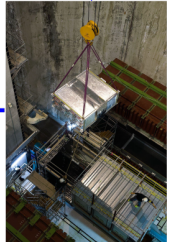


Installation of the detectors in the basket (2023/2024)

- Every detector follows the same steps:
- Delivery at JPARC in the Neutrino Assembly building
- Transportation of the detector into the Neutrino Monitoring building
- Lowering of the detectors inside the pit (33 m deep)
- Installation inside the basket



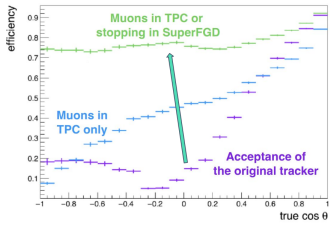


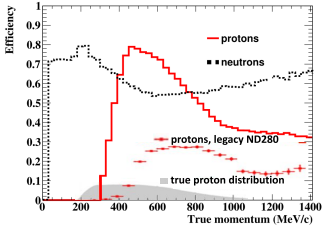


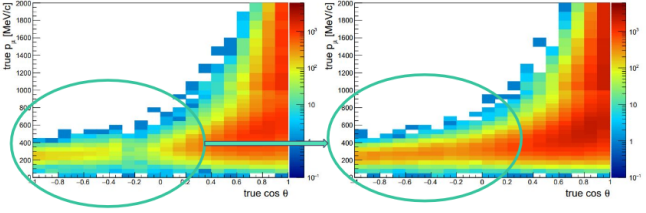


Improvements thanks to the upgrade

- High muon detection efficiency for all angles
- Proton reconstruction:
  Lower threshold
  Improved energy resolution
- Higher detection efficiencies
- Fully reconstruct final state event kinematics especially by detecting the neutrons

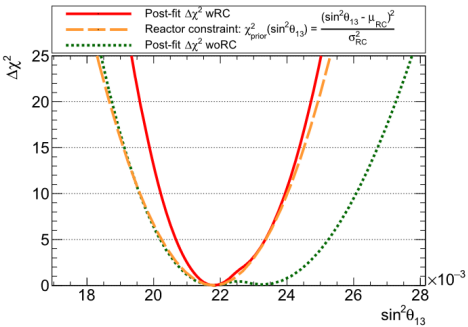


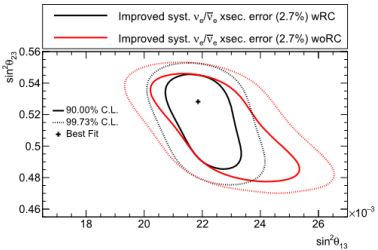


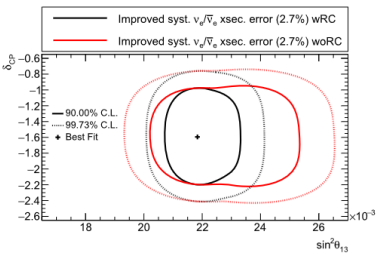


From T2K to HK

- Entering precision neutrino physics era
- Higher statistics with much larger fiducial mass
- Improved near-detector acceptance with upgraded ND280
- Water-Cherenkov ND: IWCD complementing ND280
- Improved ν_e constraints: cross-section uncertainties
- More demanding systematics control
- 5σ-CPV discovery in less than three years if maximal CPV and known MO



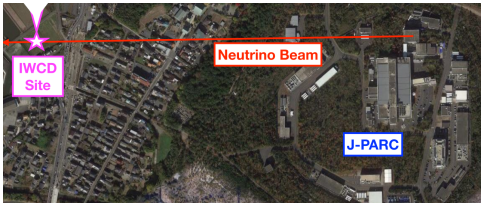


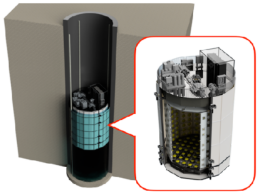


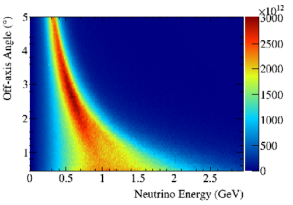
Eur. Phys. J. C (2026) 86:170

IWCD: Intermediate Water Cherenkov Detector

- Detector located $\sim$ 850 m from neutrino source
- 45 m deep pit in which detector moves
- Measurements of ν_e flux and cross-section before oscillation
- Same technology as far detector to reduce detector effects
- Unique capability to probe neutrino energy with off-axis angle dependence of beam







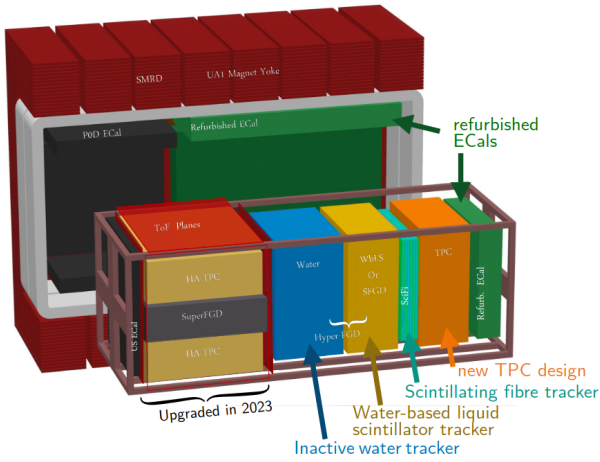
Hyper-Kamiokande status

- Hyper-Kamiokande cavern completed in June 2025
- Tank lining is in progress and will be completed soon
- PMT testing and assembly above ground has already started
- Construction is scheduled to be completed in JFY 2027
- Beginning of data taking scheduled for end of 2028
- Neutrino beam data taking scheduled in early 2029



Further upgrading ND280: ND280++ (2032)

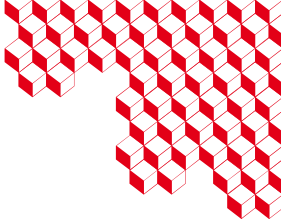
- Requirements for the high-statistics phase:
- Better constraint on $\nu_e/\bar{\nu}_e$ cross-section ratio
- Same atom for neutrino interaction at ND and FD
- Large fiducial mass to complement IWCD
- Precise hadron reconstruction and tracking for neutrino-nucleus interactions
- R&D towards several detector designs
- Ongoing sensitivity studies towards a Conceptual Design Report (2027)



Conclusions

- ND280 detector upgrade is complete
- Systematic uncertainties reduction $\Rightarrow$ improve oscillation parameters and search for CP violation
- Improved performance: muon angle coverage, proton efficiency, neutron detection
- Beam upgrade ongoing up to 1.3 MW for HK
- T2K will stop data taking in June 27
- Hyper-Kamiokande cavern excavated and ready for construction
- Data taking to start by end of 2028, neutrino beam run early 2029





Thank you !

CEA SACLAY
91 191 Gif-sur-Yvette Cedex
France
guillaume.eurin@cea.fr

Additional slides

Why a near detector?

Total **uncertainties** on ν_μ 1Ring at SK (largest sample) reduced from 17% to **3%** thanks to **ND constraints**.
Perfect propagation from ND to FD limited by:

- lower high-angle acceptance
- scalability of cross sections between different materials (C vs O)
- detection thresholds

Detected muon neutrinos at FD

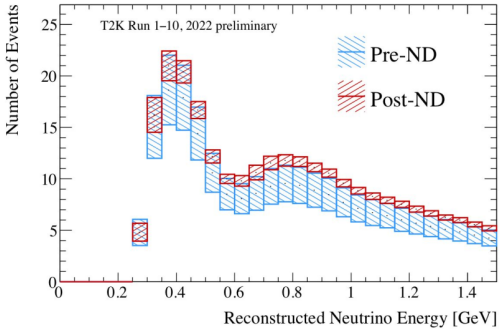
ν_μ survival probability

$$N_\mu(E_\mu) \propto P(\nu_\mu \to \nu_\mu)\,\sigma(E_\nu)\,\Phi_{\nu_\mu}(E_\nu)$$

Cross section, from ND and other measurements

ν flux, from ND and beam measurements

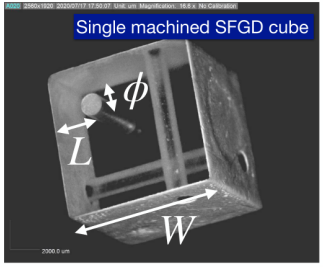
Same formula used for ν_e appearance

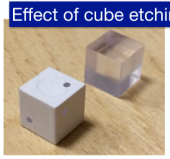


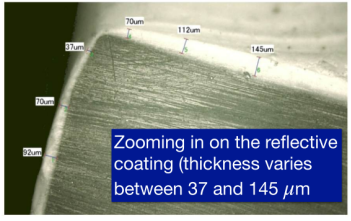
SK neutrino mode 1R muon sample spectrum before and after ND fit [arXiv:2303.03222]

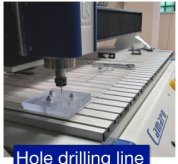
E. Villa - WIN 2025

Super Fine Grained Detector cubes









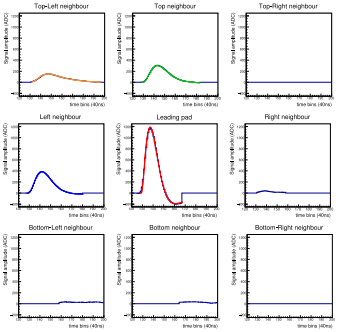
- Single SFGD cube - polystyrene with 1.5% paraterphenyl (PTP) and 0.01% POPOP, produced by the UNIPLAST Co. (Vladimir, Russia) by injection moulding (4,000 cubes per day during production process)
- Channels drilled into the cubes for optical fibre feed-through (12,000 holes drilled per day to keep up with manufacturing rate)
- Up to 5 drilling machines and 13 operators used at full production rate
- Reflective layer introduced by chemical etching the cubes (micro-porosity makes the surface appear white)
- Dimensions after etching:
  $L = (2.88 \pm 41)$ mm, $W = (10.16 \pm 0.06)$ mm
  ($\phi \sim 1.4$ mm stainless steel rods used to mechanically reject cubes with badly drilled holes)
- Low tolerances for cube dimensions are crucial for detector assembly (~2,000,000 cubes)

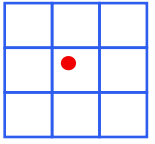
Signal modelling - (NIM-A.2023.168534)

- $Q_{pad}(t)$ = Solution of 2D Telegraph equation for diffusion of initital Q_e deposited charge (point-like, delta-pulse initial conditions)

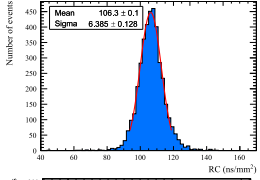
$$Q_{pad}(t) = \frac{Qe}{4} \times \left[erf(\frac{x_{high} - x_0}{\sqrt{2}\sigma(t)}) - erf(\frac{x_{low} - x_0}{\sqrt{2}\sigma(t)}) \right] \times \left[erf(\frac{y_{high} - y_0}{\sqrt{2}\sigma(t)}) - erf(\frac{y_{low} - y_0}{\sqrt{2}\sigma(t)}) \right], \sigma(t) = \sqrt{\frac{2t}{RC}}$$

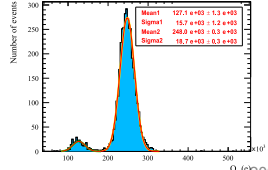
- Current induced on a pad $\frac{dQpad(t)}{dt}$ convoluted with electronics transfer function R(t)
- Simultaneous fit of waveforms of leading pad + neighbouring pads





RC, Gain

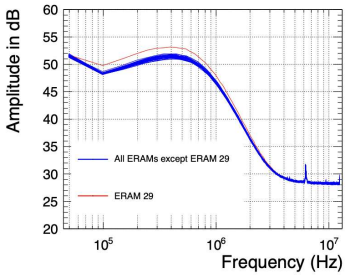


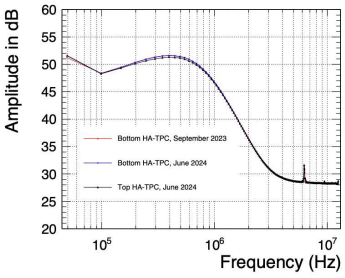


Noise Study

https://doi.org/10.1016/j.nima.2025.

Mean Fast Fourier Transform Spectrum

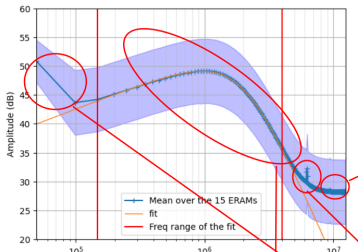


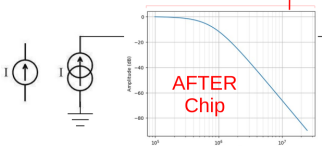


- The analysis is based on data collected from 32 ERAM detectors, recorded without zero suppression.
- The spectra of the different ERAMs are remarkably similar and stable over time, except for ERAM 29, which exh a higher noise amplitude. The capacitance of ERAM 29 is twice that of the other detectors→ its higher capacitan leads to increased noise (ERAM 29 features half the glue thickness and half the surface resistivity)
- The nearly identical noise levels across all ERAMs reflect :
  - the excellent uniformity of the electronics and the mechanical definition of the glue layer driving the detector capacitance.

Noise modelisation

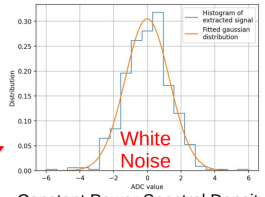
- Various noise populations identified
- Result of the work of numerous students and staff
- Accurate description of the noise in the simulation





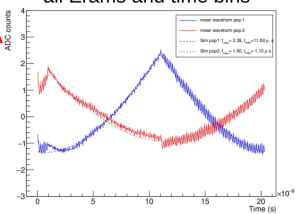
The Bulk of the spectrum

$$ADC(t) = I_{input} \otimes AFTER_{pulse}$$

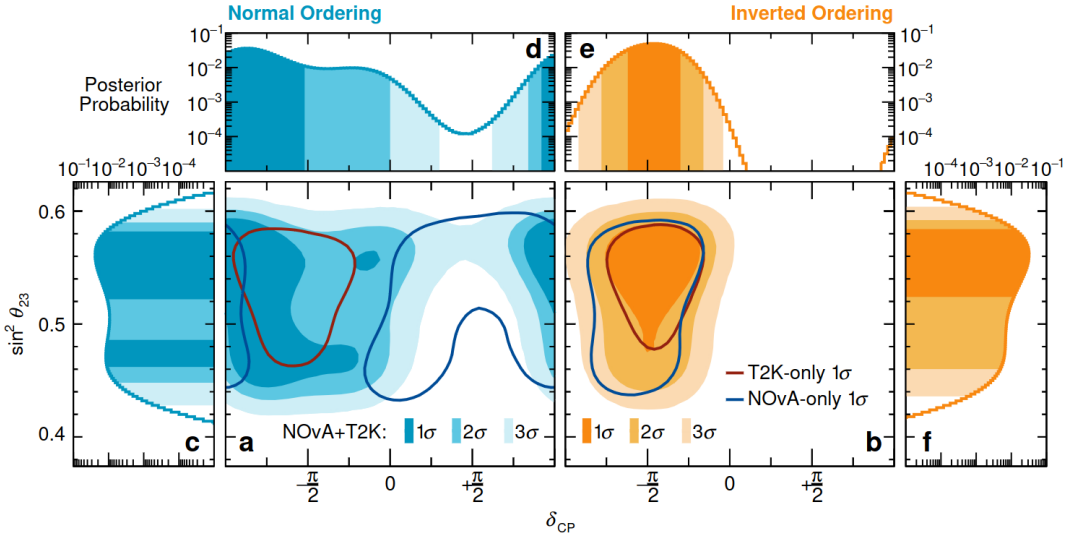


Constant Power Spectral Density
σ ~1 ADC

Averaged waveform over all Erams and time bins



T2K-Nova joint fit



Nature volume 646, pages 818–824 (2025)